Safe grounding system design for a photovoltaic power station

Zacharias G. Datsios and Pantelis N. Mikropoulos

***Abstract*--A safe and cost-efficient grounding system design of a 3 MWp photovoltaic power station according to IEEE Std 80-2000 is presented. Grounding analysis is performed by considering the metal parts of the photovoltaic panel arrays foundations as auxiliary ground electrodes. Utilizing also horizontal ground conductors, required solely for the interconnections of the metal support structures of the photovoltaic panel arrays, both safety and cost-efficiency in grounding system design have been achieved. It is shown that in large-scale photovoltaic power stations where the metal parts of the panel arrays foundations are concrete encased the concrete resistivity is not an important parameter in evaluating the safety performance of the grounding system.**

***Index Terms*--grounding system design, photovoltaic power station, safety, touch and step voltages.**

I. Introduction

The safe grounding system design of a technical installation is based on the protection of persons against the danger of critical electric shock. Furthermore, it allows for the flow of normal or fault currents into the earth without exceeding operating and equipment limits or affecting adversely the continuity of service [1]. A safe grounding system design requires the calculation of allowable touch and step voltage limits which should not be exceeded, as well as the computation of the ground resistance, the ground potential rise and of the touch and step voltages arising in case of the worst possible ground fault. These design parameters depend on the soil resistivity of the installation area. Thus, initially, accurate soil resistivity measurements at the site of the planned installation should be performed.

In general, the design procedure of a safe grounding system consists of five major steps:

i. Analysis of soil resistivity measurements
ii. Estimation of the allowable limits of touch and step voltages
iii. Fault current analysis for the estimation of the maximum grid current
iv. Grounding system design
v. Evaluation of the safety performance of the designed grounding system.

In recent years the use of renewable energy sources, such as wind and solar power, for the generation of green electrical energy has increased rapidly. Numerous large-scale photovoltaic power stations covering large areas and yielding power higher than 500 kWp have already been constructed around the globe and more are planned. According to [2], large-scale photovoltaic power stations installed worldwide during 2010 yield power about 3.5 GWp and the total installed power is higher than 9 GWp. Despite the rapid increase in the number of photovoltaic power stations, their safe grounding system design is analyzed sparsely in literature [3]. This paper presents the safe and efficient grounding system design of a 3 MWp photovoltaic power station. The grounding design is carried out according to the IEEE Std 80-2000 [1], which is primarily concerned with outdoor ac substations. However, as discussed in this work, a photovoltaic power station differs from a typical outdoor ac substation, introducing, therefore, a number of issues related to grounding analysis.

II. Photovoltaic Power Station Under Study

Fig. 1 illustrates the 3 MWp photovoltaic power station under study which comprises 12 photovoltaic panel array groups and covers an area of about 58000 m^2. The generated power is collected at three local prefabricated substations, transferred by underground high voltage cables to the main indoor substation and finally delivered to the 20 kV distribution system. The metal structures of the photovoltaic

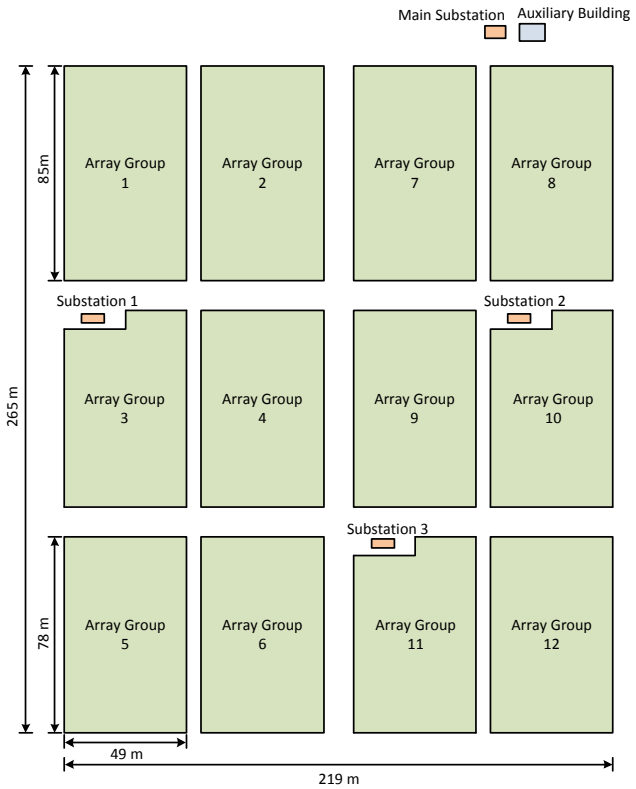

Fig. 1. Layout of the 3 MWp photovoltaic power station under study.

Z. G. Datsios (e-mail: zdatsios@auth.gr) and P. N. Mikropoulos (e-mail: pnm@eng.auth.gr) are with the Department of Electrical Energy, School of Electrical and Computer Engineering, Aristotle University of Thessaloniki, Thessaloniki, 54124 Greece.

panel arrays are supported by hot-dip galvanized steel piles with buried cast-in-place concrete foundations with an outer concrete diameter of 0.23 m; the length of the concrete encased part of the piles is 1.1 m.

III. Analysis of Soil Resistivity Measurements

It is well known that soil resistivity varies through the year due to the changes in the moisture content and temperature mostly of the upper soil layers. Generally, soil resistivity increases with decreasing moisture content and temperature. When temperature drops below the freezing point, the water in the soil freezes and soil resistivity rises abruptly [1], [4]-[7]. The highest values of soil resistivity are obtained in prolonged dry periods of the year due to the low moisture content of the soil or in the winter when the water in the upper soil layers is frozen. Therefore, the time of soil resistivity measurements should be selected properly so as to obtain conservative results.

Several soil resistivity measurement methods exist [7] with the Wenner four-pin method [8] being widely used. According to this method, four electrodes are driven into the soil to a depth b at equal distances α apart in a straight line (Fig. 2). The test current is injected into the earth via the two outer electrodes and the arising voltage is measured between the two inner electrodes. The measured voltage is divided by the test current and a resistance value is obtained. For the calculation of the apparent soil resistivity, ρ (Ωm), the following approximate expression is used when the depth b is considerably smaller than the distance between adjacent electrodes α [7], [8]

$$\rho = 2\pi\alpha R \tag{1}$$

where α (m) is the spacing between adjacent electrodes and R (Ω) is the obtained resistance. The larger the spacing between adjacent electrodes, the deeper the test current penetrates the soil. Thus, the measured soil resistivity is considered as the apparent soil resistivity to a depth equal to the electrode spacing [1]. As soil resistivity is rarely uniform and commonly varies with depth, soil resistivity should be measured for several electrode spacing values. Initially, a small spacing should be used to measure the soil resistivity of surface layers. Subsequently, the spacing should be increased to larger values for the determination of the soil resistivity of deeper layers.

The interpretation of the soil resistivity measurements and the derivation of a representative soil model approximating the actual soil conditions is a difficult task. Generally, soil models can be divided into three categories: uniform, two-layer and multilayer soil models. Uniform soil models can be used only when the actual soil is practically homogeneous, something that is not common in practice [1]. Non-uniform soil conditions can be represented by two-layer soil models, which comprise an upper layer of a finite depth, h (m), and resistivity, ρ_1 (Ωm), and a lower layer of different resistivity, ρ_2 (Ωm), and infinite thickness. Normally, these models are sufficiently accurate in representing the actual non-uniform soil conditions for safe grounding system design purposes [1]. This does not apply when the apparent resistivity as a function of electrode spacing exhibits several local extrema, i.e. the soil is highly non-uniform; in such cases a multilayer soil model should be employed. The relevant IEEE Standards [1], [7] propose several methods for the interpretation of soil resistivity measurements, including analytical methods and graphical methods, such as Tagg's [6] or Sunde's [9].

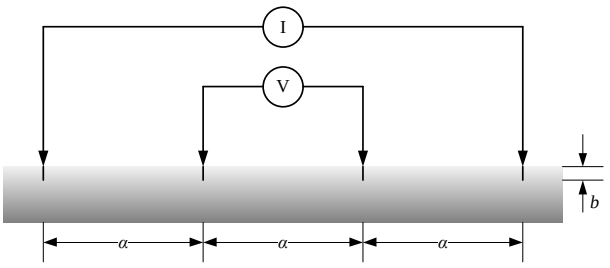

Fig. 2. Wenner four-pin method electrode arrangement [8].

Soil resistivity measurements at the installation site of a large-scale photovoltaic power station should be carried out for several values of electrode spacing, including large spacings for the estimation of the soil resistivity of larger depths. Moreover, lateral changes of the soil resistivity should be evaluated as well, so several positions in the vast installation area should be selected. For the photovoltaic installation under study, soil resistivity measurements were performed, according to the Wenner method [8], at eight different positions within the site of installation and with electrode spacings of 2, 4, 8, 16 and 32 m; the average values of the measured apparent soil resistivity are listed in Table I. As the apparent soil resistivity generally increases with increasing electrode spacing (Table I), a two-layer soil model can represent satisfactorily the actual soil conditions. Results were analyzed with the soil analysis module of the CYMGrd software [10], which uses an expression proposed by Tagg [6] correlating the apparent resistivity with electrode spacing and employs computational methods to minimize an error function in order to obtain the optimal two-layer soil model. The variation of the apparent soil resistivity with the electrode spacing together with the two-layer soil model (ρ_1=2796 Ωm, ρ_2=7250 Ωm, h=4.45 m) are shown in Fig 3.

TABLE I
Measured Apparent Soil Resistivity

Electrode Spacing (m)	Apparent Soil Resistivity (Ωm)
2	3028
4	2944
8	4507
16	5298
32	6429

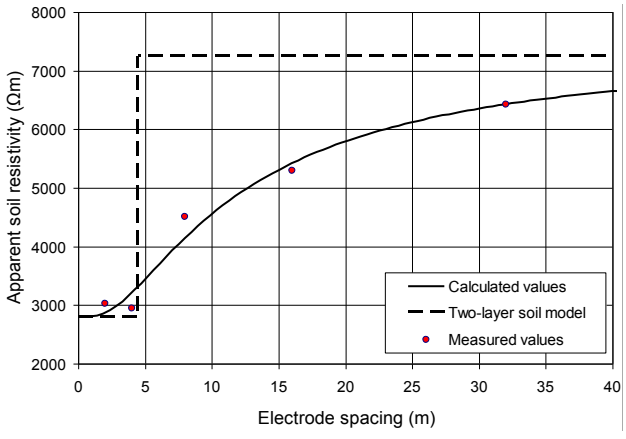

Fig. 3. Variation of the apparent soil resistivity with electrode spacing and the two-layer soil model derived by using the CYMGrd software [10].

IV. Estimation of the Allowable Limits of Touch and Step Voltages

The estimation of the maximum allowable touch and step voltages is required for the safe design of a grounding system. These voltage limits are derived from the tolerable body currents which do not cause ventricular fibrillation and depend on the soil resistivity and the duration of the shock current to which a person might be exposed; the latter corresponds to the fault clearing time of primary protection or to that of the slower backup protection [1]. The touch and step voltages caused by ground faults should be lower than the allowable touch and step voltage limits, respectively.

The allowable limits of touch and step voltages, E_{touch} (V) and E_{step} (V), respectively, are given as [1]

$$E_{touch} = \left(1000 + 1.5C_s \cdot \rho_s\right)\left(k/\sqrt{t_s}\right) \quad (2)$$

$$E_{step} = \left(1000 + 6C_s \cdot \rho_s\right)\left(k/\sqrt{t_s}\right) \quad (3)$$

where t_s (s) is the duration of the shock current and k is a factor equal to 0.116 or 0.157 for people with body weight of 50 kg and 70 kg, respectively [1]. C_s is a derating factor, given by (4) [1], introduced when a thin layer of high resistivity surface material is spread on the earth's surface within the installation area in order to increase the contact resistance between the ground and persons' feet.

$$C_s = 1 - \frac{0.09\left(1 - \frac{\rho}{\rho_s}\right)}{2h_s + 0.09} \quad (4)$$

In (4) ρ (Ωm) and ρ_s (Ωm) are the soil and surface material resistivities, respectively and h_s (m) is the thickness of the surface material. If no surface material is applied, then ρ_s is equal to ρ and C_s is equal to 1. It is important to note that the surface material resistivity corresponding to wet conditions should be used in calculations in order to obtain results on the side of safety.

According to common practice, photovoltaic power stations are usually protected by fences and are inaccessible to the general public. Thus, the allowable voltage limits obtained for a person weighing 70 kg should be selected for the installation area. On the other hand, for areas outside the fence, the allowable limits obtained for a person weighing 50 kg may be selected as well. Furthermore, it should be pointed out that the application of a high resistivity surface material is not common in photovoltaic installations. However, such surface material may be spread on certain restricted areas of the installation, as a cost-effective method to achieve safety.

Table II shows the calculated allowable touch and step voltage limits of the installation under study as a function of the surface material resistivity for three different durations of shock current and with a surface material thickness of 0.15 m. As expected, the allowable touch and step voltage limits are higher for a person with body weight of 70 kg than 50 kg, increase with increasing surface material resistivity and decrease as the duration of shock current increases. In this study, the selected limits of touch and step voltages are 1153 V and 3947 V, respectively, corresponding to a person weighing 70 kg, a duration of shock current of 0.5 s and no surface material application.

TABLE II
Allowable Touch and Step Voltages Limits Calculated According to (2)-(4); Surface Material Thickness 0.15 m

ρ_s (Ωm)	t_s (s)					
	0.1		0.5		1	
	$E_{touch70}$ (V)	E_{step70} (V)	$E_{touch70}$ (V)	E_{step70} (V)	$E_{touch70}$ (V)	E_{step70} (V)
without	2579	8825	**1153**	**3947**	815	2791
4000	3268	11584	1462	5181	1034	3663
5000	3841	13876	1718	6205	1215	4388
6000	4414	16167	1974	7230	1396	5112
7000	4987	18459	2230	8255	1577	5837
8000	5560	20750	2486	9280	1758	6562
9000	6133	23041	2743	10304	1939	7286
10000	6706	25333	2999	11329	2120	8011
	$E_{touch50}$ (V)	E_{step50} (V)	$E_{touch50}$ (V)	E_{step50} (V)	$E_{touch50}$ (V)	E_{step50} (V)
without	1905	6521	852	2916	603	2062
4000	2415	8559	1080	3828	764	2707
5000	2838	10252	1269	4585	898	3242
6000	3261	11945	1459	5342	1031	3777
7000	3685	13638	1648	6099	1165	4313
8000	4108	15331	1837	6856	1299	4848
9000	4531	17024	2026	7613	1433	5384
10000	4954	18717	2216	8371	1567	5919

V. Estimation of the Maximum Grid Current

For the safe grounding system design, fault current calculations should be performed so as to determine the most dangerous ground fault, which is usually associated with the highest value of grid current. The latter is defined in [1] as the portion of the symmetrical ground fault current that flows between the grounding grid and the surrounding earth. The rms value of the symmetrical grid current, I_g (A), is given as [1]

$$I_g = S_f \cdot I_f \quad (5)$$

where I_f (A) is the rms value of the symmetrical ground fault current and S_f is the fault current division factor. S_f is lower or equal to unity and takes into account the portion of the symmetrical ground fault current flowing away from the grounding grid through overhead ground wires, neutral conductors, counterpoise conductors, buried metal pipes and cables with sheaths or armor in contact with the soil.

However, the actual fault current is usually asymmetrical. Thus, an rms equivalent of the actual grid current shall be estimated in order to take into account the asymmetry of the fault current in the grounding system design. This rms equivalent current, called maximum grid current, I_G (A), is given as [1]

$$I_G = D_f \cdot I_g \quad (6)$$

where D_f is a decrement factor introduced so as to consider the dc offset of the asymmetrical fault current. This factor depends on the duration of the fault, t_f (s), and the *X/R* ratio, which is the ratio of inductive reactance to resistance of the system at the fault location, indicating the rate of the dc offset decay. The decrement factor, D_f, is given as [1]

$$D_f = \sqrt{1 + \left(T_a/t_f\right) \cdot \left(1 - e^{-2t_f/T_a}\right)} \quad (7)$$

where the dc offset time constant T_a (s) is equal to $X/(\omega R)$.

The most dangerous ground fault for a photovoltaic power station typically corresponds to a ground fault at the high voltage side of the step-up transformers. However, exceptions may occur, as in [3], where the worst ground fault occurs at the switching station of a power plant adjacent to the photovoltaic power station. In the present photovoltaic power station the worst ground fault generating the highest grid current corresponds to a 20 kV single phase ground fault at the main substation. The value of 1 kA for the symmetrical ground fault current, I_f, was considered as a worst case scenario; the ground fault currents at the 20 kV side of the step-up transformers are limited to values lower than 1 kA by the 12 Ω current limiting resistance utilized in the particular medium voltage distribution system. The fault current division factor, S_f, was taken equal to 1, since no overhead ground wires or neutral conductors exist; therefore the symmetrical grid current I_g equals to 1 kA according to (5). The decrement factor, D_f, was found 1.0127, calculated according to (7) for a *X/R* ratio equal to 4 and a fault duration of 0.5 s corresponding to the fault clearing time of the primary protective devices. Hence, the maximum grid current, I_G, used for the grounding system design was found 1012.7 A according to (6).

VI. Grounding System Design

In order to ensure a safe, yet cost-efficient, grounding system design for a photovoltaic power station, the metal parts of the foundations supporting the metal structures of the photovoltaic panel arrays should be considered as auxiliary ground electrodes. This is essential as it reduces considerably the photovoltaic power station's ground resistance and, consequently, the ground potential rise and the arising touch and step voltages within the installation in case of a ground fault. Hence, both safety and cost-efficiency can be achieved without requiring excessively large lengths of ground conductors or a high resistivity surface material spread to the whole installation area of the photovoltaic facility.

A large number of different foundation types can be utilized to support the metal structures of the photovoltaic panel arrays. From the grounding system design point of view, they can be divided into those with metal parts in direct contact with the soil, e.g. driven piles and ground screws, and those with concrete encased metal parts, e.g. concrete encased piles and concrete foundations with steel reinforcing bars. The cross section of the metal parts of these foundation types is normally large enough to carry the ground fault currents into the earth. This also applies for the metal structures which support the photovoltaic panels and interconnect the metal parts of the foundations. Nevertheless, attention should be given to the interconnections of the metal structures because paint films, protective coatings and metal surface treatments could introduce high resistances, resulting in unreliable electrical connections.

Concrete encased electrodes were first used as ground electrodes for lightning protection systems of military installations in the 1940s [11]. Concrete is a hygroscopic material that means it attracts moisture from the surrounding soil [1], [12] and therefore it retains a high water content and low resistivity even under adverse conditions [12]. The IEEE Std 80-2000 [1] proposes for the resistivity of concrete values ranging between 30 Ωm and 90 Ωm. However, several authors, based on literature review, have proposed higher values for concrete resistivity, such as 100-300 Ωm [13] and 100-400 Ωm [14]. It is noteworthy that the ground resistance of concrete encased electrodes is lower than the ground resistance of the same electrodes embedded directly in soil when the resistivity of the latter is relatively high [1].

For the photovoltaic power station under study the concrete encased parts of the hot-dip galvanized steel piles supporting the photovoltaic panel arrays were considered as auxiliary ground electrodes. The 28 piles belonging to each photovoltaic panel array (Fig. 4) are all interconnected above ground by the metal structures supporting the photovoltaic panels. Also, horizontal ground conductors, buried next to the array groups at a depth of 0.5 m, were employed to interconnect the metal support structures of all photovoltaic panel arrays, as shown for the array groups 1 and 2 in Fig. 4.

The grounding systems of the substations and of the auxiliary building consist of a foundation earth electrode and a ring ground electrode being buried at a depth of 0.5 m and surrounding the buildings at a distance of 1 m from their boundaries. These grounding systems are connected to the photovoltaic power station's grounding network with two horizontal ground conductors buried at 0.5 m.

All the ground conductors are made of copper-clad steel and have the commercially available diameter of 10 mm. It must be noted that the minimum conductor size based on fusing was calculated 5.36 mm^2 according to [1] for the maximum grid current of 1012.7 A and for the fault clearing time of 1 s corresponding to the backup protection.

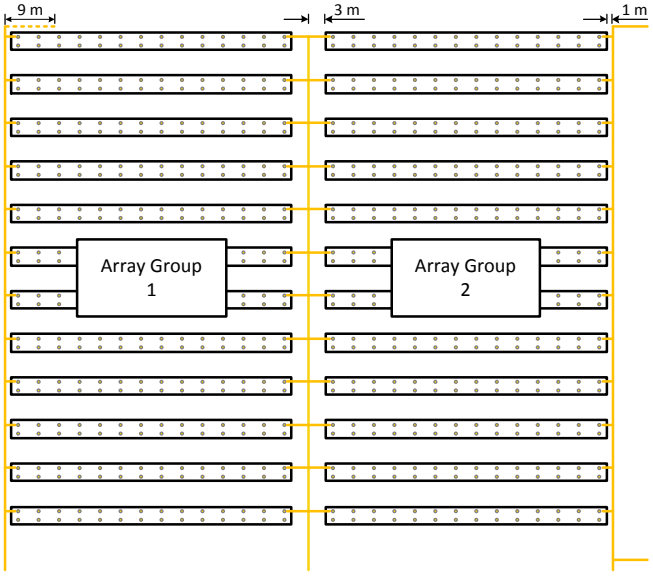

Fig. 4. Schematic of the grounding system of array groups 1 and 2. Circles represent the piles supporting the metal structures of the photovoltaic panel arrays. Yellow lines depict horizontal ground conductors buried at 0.5 m.

VII. Safety Performance Evaluation

The safety performance of the grounding system was evaluated with the aid of the CYMGrd software [10]. Fig. 5 shows the computer model of the photovoltaic power station's grounding system. The model includes 3766 concrete encased steel piles, arranged according to the exact

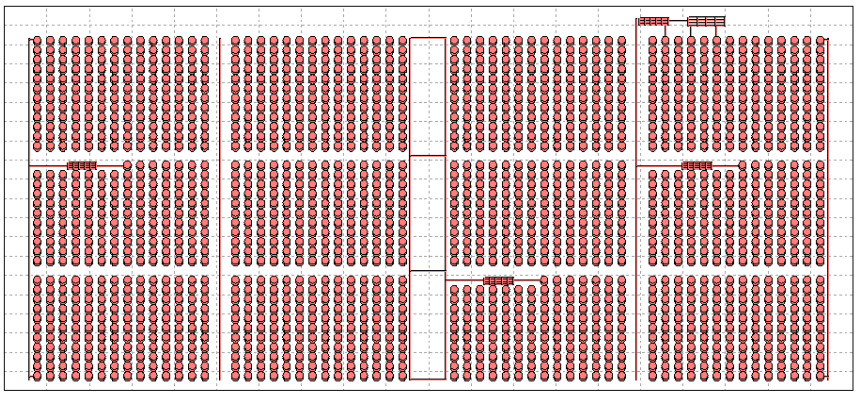

Fig. 5. Computer model of the photovoltaic power station's grounding system. The graph is not according to scale.

layout of the photovoltaic panel arrays, and approximately 1.7 km of buried horizontal ground conductors. The connections of the horizontal ground conductors with the adjacent piles were not modeled except for those at the outer corners of the photovoltaic facility, where the highest touch and step voltages are typically expected; this would result in conservative results. The foundation earth electrodes of the substations and the auxiliary building were modeled as sparse grounding grids. The concrete resistivity was assumed equal to 90 Ωm, which the highest value proposed by the IEEE Std 80-2000 [1]. It must be mentioned that the CYMGrd software [10] assumes that all the electrodes are electrically connected together and are elevated to a single potential, the ground potential rise.

It was not possible to analyze the complete computer model of the photovoltaic power station's grounding system (Fig. 5) due to the large number of piles employed; this is common for large-scale photovoltaic power stations. To overcome this limitation, the number of the modeled piles could be reduced appropriately. However, the exact layout of the piles should always be maintained in the areas where the safety performance of the grounding system is evaluated. Nevertheless, the modified computer model would yield results on the side of safety due to the reduced number piles employed in analysis. As an alternative approach [3], the modeled piles, with the exception again of those positioned at the areas where the safety performance is evaluated, could be replaced by sparse horizontal ground conductors, obtaining, thus, conservative results.

In the present case, the computer model of the photovoltaic power station's grounding system (Fig. 5) was divided in two sections A and B comprising array groups 1-6 and 7-12, respectively (Fig. 1). Subsequently, the number of the modeled piles in section A was reduced appropriately and safety performance was evaluated in section B and vice versa. For both cases, the ground resistance and ground potential rise were found approximately 11.9 Ω and 12 kV, respectively; according to above, these are conservative values, resulting, therefore, in a safer grounding design.

Fig. 6 shows touch voltage contours for the section A of the computer model of the photovoltaic power station's grounding system; the number of the modeled piles was reduced appropriately in section B. From Fig. 6 it can be seen that, with the exception of the two outer corner areas of the photovoltaic facility, the touch voltages computed for distances up to 1 m from the photovoltaic panel arrays' and substation's metal structures are well below the corresponding 1153 V touch voltage limit. This is also true for the section B of the computer model, where the highest touch voltage (1486 V) within the installation area is found at the outer corner of the array group 12 (Fig. 1). In order to ensure safety in the four outer corner areas of the photovoltaic installation, a surface material with resistivity equal to or higher than 5000 Ωm (Table II) can be used locally to increase the allowable touch voltage limit (≥1718 V) above the computed touch voltages. Otherwise, a short horizontal ground conductor with length about 9 m can be installed at each outer corner area, parallel to the last photovoltaic panel array at a distance of 1 m from its boundary, as depicted in Fig. 4 for array group 1. Fig. 7 shows the touch voltages computed along a profile parallel to the outermost array of the facility in array group 12 (Fig. 1) at a distance of 1 m from its metal structure for the cases

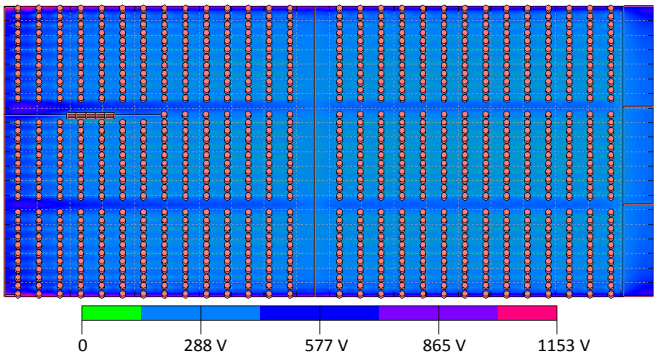

Fig. 6. Touch voltage contours of computer model section A. The graph is not according to scale; the highest touch voltage is 1485 V.

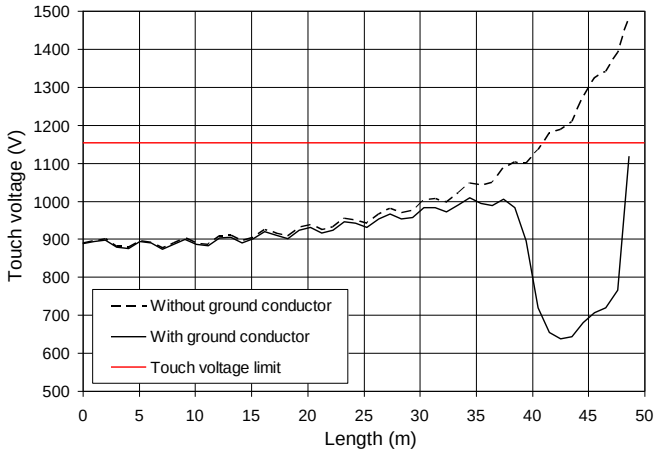

Fig. 7. Touch voltages computed along a profile parallel to the outermost array of the photovoltaic facility in array group 12 at a distance of 1 m from its metal structure; cases of with and without the 9 m horizontal ground conductor, red line depicts the touch voltage limit of 1153 V.

of with and without the horizontal ground conductor. It is obvious that the addition of the short ground conductor reduces the computed touch voltages to values lower than the touch voltage limit.

The maximum computed surface potential difference within the installation area is 3655 V. Thus, the step voltages being lower than the 3947 V step voltage limit (Table II), are not a threat for persons in the installation area.

Summarizing, as the computed touch and step voltages arising in the photovoltaic facility in case of the worst possible ground fault are lower than the allowable limits of touch and step voltages, the designed grounding system ensures the safety of persons in the installation area.

Finally, analysis of the photovoltaic facility's grounding system was also performed for different values of concrete resistivity, ranging from 30 Ωm to 400 Ωm. The limits of this range correspond to the lowest and highest values of concrete resistivity proposed in [1], [12] and [14]. The effect of concrete resistivity on ground resistance, thus also ground potential rise, was found to be negligible, as the ground resistance varied less than 1.5% over the range of concrete resistivity studied. Actually, the ground resistance increased only slightly (12.05 Ω) when the pile concrete encasement was disregarded in analysis, in spite of the relatively high resistivity of the upper soil layer (2796 Ωm). This is because of the large number of ground electrodes in the installation area; in such cases, the resistivity of the concrete encasing ground electrodes is not an important parameter in evaluating the safety performance of the grounding system.

VIII. Conclusions

A safe and cost-efficient grounding system of a 3 MWp photovoltaic power station has been designed according to IEEE Std 80-2000 with the aid of grounding analysis software. The metal parts of the photovoltaic panel arrays foundations should be considered as auxiliary ground electrodes. In this case, by utilizing also horizontal ground conductors required solely for the interconnections of the metal support structures of the photovoltaic panel arrays rather than forming a mesh, both safety and cost-efficiency in grounding system design are achieved. In restricted areas, mainly at the outer boundaries of the photovoltaic panel array groups, where touch voltages exceed the allowable limit, a high resistivity surface material can be spread or horizontal ground conductors of relatively short lengths can be added.

Grounding analysis of large-scale photovoltaic power stations, involving a large number of ground electrodes, can be performed by reducing the number of the ground electrodes in the computer model, provided that their exact layout is always maintained in the areas where the safety performance of the grounding system is evaluated. Such a modified computer model yields a higher ground resistance, due to the reduced number of ground electrodes employed in analysis, however results are on the side of safety.

In large-scale photovoltaic power stations where the metal parts of the panel arrays foundations are concrete encased the concrete resistivity does not affect appreciably the ground resistance, thus it is not an important parameter in evaluating the safety performance of the grounding system.

IX. References

[1] *IEEE Guide for Safety in AC Substation Grounding*, IEEE Std 80-2000, Jan. 2000.

[2] "PV Power Plants 2011-Industry Guide", Renewables Insight (RENI), 2011.

[3] J. Ma and F. P. Dawalibi, "Grounding analysis of a solar power generation facility," in *Proc. 2010 Asia-Pacific Power and Energy Engineering Conference (APPEEC)*, Chengdu, China, Mar. 2010.

[4] P. J. Higgs, "An investigation of earthing resistances," *Journal of the IEE*, vol. 68, no. 402, pp. 736-750, Jun. 1930.

[5] R. Rüdenberg, "Grounding principles and practice I-Fundamental considerations on ground currents," *Electrical Engineering*, vol. 64, no. 1, pp. 1-13, Jan. 1945.

[6] G. F. Tagg, "Earth resistances," Pitman Publishing Corporation, London, 1964.

[7] *IEEE Guide for Measuring Earth Resistivity, Ground Impedance, and Earth Surface Potentials of a Ground System Part I: Normal Measurements*, ANSI/IEEE Std 81-1983, 1983.

[8] F. Wenner, "A method of measuring earth resistivity," *Bulletin of the Bureau of Standards*, Scientific Paper 258, vol. 12, pp. 469-478, Jul. 1915.

[9] E. D. Sunde, "Earth conduction effects in transmission systems," Dover Publications Inc, New York, 1968.

[10] CYMGRD 6.3 for Windows "User's guide and reference manual," CYME International T&D Inc., Oct. 2006.

[11] H. G. Ufer, "Investigation and testing of footing-type grounding electrodes for electrical installations," *IEEE Trans. Power App. Syst.*, vol. PAS-83, no. 10, pp. 1042-1048, Oct. 1964.

[12] E. J. Fagan and R. H. Lee, "The use of concrete-enclosed reinforcing rods as grounding electrodes," *IEEE Trans. Ind. Gen. Appl.*, vol. IGA-6, no. 4, pp. 337-348, Jul./Aug. 1970.

[13] J. Preminger, "Evaluation of concrete-encased electrodes," *IEEE Trans. Ind. Appl*., vol. IA-11, no. 6, pp. 664-668, Nov./Dec. 1975.

[14] A. M. Mousa, "Discussion of "Fault induced voltages on metallic fencing located in the vicinity of a high voltage substation," *IEEE Trans. Power App. Syst.*, vol. PAS-101, no. 3, pp. 746-750, Mar. 1982".

X. Biographies

Zacharias G. Datsios was born in Kozani, Greece, in 1986. He received the M.Eng. degree in electrical and computer engineering from Aristotle University of Thessaloniki (AUTh), Thessaloniki, Greece, in 2010, where he is currently pursuing the Ph.D. degree at the High Voltage Laboratory. His research is related to grounding systems, especially dedicated to the soil ionization phenomenon.

Pantelis N. Mikropoulos was born in Kavala, Greece, in 1967. He received the M.Eng. and Ph.D. degrees in electrical and computer engineering from Aristotle University of Thessaloniki (AUTh), Thessaloniki, Greece, in 1991 and 1995, respectively.

He held postdoctoral positions at AUTh and the University of Manchester, Manchester, UK. He was Senior Engineer with Public Power Corporation SA, Athens, Greece. He was elected Assistant Professor and Associate Professor in High Voltage Engineering at AUTh in 2003 and 2010, respectively. Since 2005 he has been the Director of the High Voltage Laboratory at AUTh. His research interests include the broad area of high-voltage engineering with emphasis given to air and surface discharges, electric breakdown, lightning protection and insulation coordination for power systems.